ENERGY-AWARE NODE SELECTION IN A DISTRIBUTED SENSOR NETWORK*

Qiang Le — Department of Electrical Engineering, Hampton University, Hampton, VA 23668

Lance M. Kaplan — US Army Research Laboratory, 2800 Powder Mill Road, Adelphi, MD 20783

James H. McClellan — Department of Electrical and Computer Engineering, Georgia Institute of Technology, Atlanta, GA 30332

ABSTRACT

This work develops a resource management strategy for a wireless sensor network of bearings-only sensors. Specifically, the resource manager determines which nodes actively sense and communicate during each snapshot in order to achieve a tolerable level of geolocalization accuracy while attempting to maximize the effective lifetime of the network. This work compares three energy-related metrics. The traditional metric that summarizes the energy usage over a single snapshot consists of the first metric. The other two metrics represent the current lifetimes of the currently active node set and the next active node set. These metrics can achieve load balancing of the nodes without resorting to computationally demanding non-myopic optimization. For any of the three metrics, the activation decision is performed in a decentralized manner over the active set of nodes. Each active node transmits just far enough to reach all the active nodes for information sharing and the potentially active nodes for information handoff. In determining the active set, partial network knowledge is considered. The partial network approach assumes that a node only knows the location of itself, the previous active set, and neighboring nodes. Simulations demonstrate the advantage of the current lifetime metrics over the more traditional energy based metric.

1 INTRODUCTION

Dense networks of unattended ground sensors (UGS) promise to provide an effective and affordable solution for surveillance and reconnaissance. To enhance the sustainability and survivability of the soldier and the sensor network, it is very important to develop resource management techniques so that only the most effective UGS nodes are collecting, sharing and disseminating information to the solider.

This work presents recent advances to develop the resource manager that will integrate into the decentralized data fusion architecture being developed under the ARL Advanced Sensors CTA (Filipov et al. 2004). Specifically, the resource manager determines which nodes actively sense and communicate during each snapshot in order to achieve a tolerable level of geolocalization accuracy while attempting to maximize the effective lifetime of the network. The traditional approaches to extend the lifetime are to choose nodes that minimize the energy required to communicate data (Williams et al. 2005; Chhetri et al. 2004). Unfortunately, those approaches require expensive dynamic programming over a large time horizon for the optimization objective to correspond to the UGS network lifetime.

In this work, we maximize a current-lifetime (CL) metric that is related to the number of snapshot cycles remaining in a node given that it continues to share data with the current set of active nodes. Unlike the traditional energy metric, a myopic optimization of the CL metric achieves load balancing, which directly relates to extending the effective lifetime of the network by preventing essential nodes from being over utilized too soon. The CL or nonlinear current lifetime (NCL) metric accounts for both the data sharing and the handoff when determining the current lifetime. The CL uses a factor to balance the energy usages of data sharing and handoff while the NCL does not. A fast Greedy Search to maximize the traditional energy metric, the CL or NCL under the constraint of geolocalization accuracy reduces computational complexity to $\mathbf{O}(N^2)$, and the use of Greedy Search is justified as well.

In addition, in this paper, for each energy-aware node selection approach, the activation decision is performed in a decentralized manner over the active set of nodes. Each active node transmits just far enough to reach all the active nodes for information sharing and handoff. In determining the active set, an active node optimizes energy-aware metrics under a localization accuracy constraint given knowl-

*Prepared through collaborative participation in the Advanced Sensors Collaborative Technology Alliance sponsored by the U.S. Army Research Laboratory under Cooperative Agreement DAAD19-01-2-008.

Report Documentation Page

Form Approved
OMB No. 0704-0188

1. REPORT DATE	2. REPORT TYPE	3. DATES COVERED
01 NOV 2006	**N/A**	**-**

4. TITLE AND SUBTITLE	
Energy-Aware Node Selection In A Distributed Sensor Network	5a. CONTRACT NUMBER
	5b. GRANT NUMBER
	5c. PROGRAM ELEMENT NUMBER
6. AUTHOR(S)	5d. PROJECT NUMBER
	5e. TASK NUMBER
	5f. WORK UNIT NUMBER
7. PERFORMING ORGANIZATION NAME(S) AND ADDRESS(ES) **Department of Electrical Engineering, Hampton University Hampton, VA 23668**	8. PERFORMING ORGANIZATION REPORT NUMBER
9. SPONSORING/MONITORING AGENCY NAME(S) AND ADDRESS(ES)	10. SPONSOR/MONITOR'S ACRONYM(S)
	11. SPONSOR/MONITOR'S REPORT NUMBER(S)

12. DISTRIBUTION/AVAILABILITY STATEMENT
Approved for public release, distribution unlimited

13. SUPPLEMENTARY NOTES
See also ADM002075., The original document contains color images.

14. ABSTRACT

15. SUBJECT TERMS

16. SECURITY CLASSIFICATION OF:			17. LIMITATION OF ABSTRACT	18. NUMBER OF PAGES	19a. NAME OF RESPONSIBLE PERSON
a. REPORT	b. ABSTRACT	c. THIS PAGE			
unclassified	**unclassified**	**unclassified**	**UU**	**7**	

Standard Form 298 (Rev. 8-98)
Prescribed by ANSI Std Z39-18

edge about the physical location of nodes within a radius of r_{nei}. The radius r_{nei} is a parameter for the node selection method to control whether local (r_{nei} is small) or global (r_{nei} is large) knowledge is employed.

The paper is organized as follows. Section 2 introduces the background which includes the models of the tracking filters, the energy usage model, the existing geometry-based metric, and partial network knowledge issue. And then Section 3 investigates three energy-aware multi-objective functions: traditional energy metric, CL, and NCL. Finally Section 4 shows the experiments to demonstrate the advantages of CL/NCL.

2 Background

The objective of this work is to investigate node selection algorithms to balance the tradeoff between the localization performance and tracking lifetime. A node selection algorithm, which is embedded in the resource manager, determines which set of nodes should be active at a given time. The algorithm should maintain a desirable localization performance while extending the tracking lifetime of the system. Furthermore, the algorithm is executed at each node in a distributed manner. In this distributed architecture, each node must also be capable of implementing track filters, that is Kalman Filters, to extract useful information out of the locally obtained measurements, broadcast the intermediate results, integrate them into a global state and predict the state for the next snapshot. The global predicted information including the predicted target state and the predicted error covariance is exploited in the node selection for the next snapshot.

This section first discusses the bearing measurement model and dynamic model in Kalman Filters. Then, the energy usage over a single snapshot and an existing geometry-based metric are given (Kaplan 2006a,b). Finally, we introduce the partial network knowledge.

2.1 Bearing Measurement and Dynamic Models

The bearing measurement obtained at the i-th node for a given snapshot is the true retarded bearing angle embedded in additive white Gaussian noise (Kaplan and Le 2005),

$$\hat{\theta}_i = \theta_i + \eta_i, \tag{1}$$

where θ_i is the true bearing angle (Kaplan and Le 2005) given by

$$\theta_i = \theta_{i,0} + \arcsin\left(\frac{v}{c}\sin(\theta_{i,0} - \phi)\right), \tag{2}$$

$\theta_{i,0} = \frac{P_{y,0}-S_{y,i}}{P_{x,0}-S_{x,i}}$ and the second term in (2) accounts for the propagation delay. The target position and velocity are labeled as $P_0 = [P_{x,0}, P_{y,0}]^T$ and $V = [V_x, V_y]^T$, respectively. The target state $[P_0^T, V^T]$ consists of the target position and velocity. The target speed $v = |V|$, the heading is $\phi = \arctan(V_y/V_x)$, and c is the speed of the sound, 347m/s. The i-th sensor node location is $S_i = [S_{x,i}, S_{y,i}]^T$. The measurement error η_i is zero-mean white Gaussian noise with a bearing measurement variance denoted as σ_i^2, i.e., $\eta_i \sim N(0, \sigma_i^2)$. In this paper, we assume the standard deviation $\sigma_i = 5^\circ$ for for $i = 1, 2, \ldots, N_s$, where N_s is the number of nodes. The retarded bearing angle model given by (2) is used to generate measurements in the simulations. However, the extended Kalman filter assumes that the mean measurement is the non-retarded bearing $\theta_{i,0}$.

The target is assumed to follow a constant velocity dynamical evolution given by

$$x(k+1) = Fx(k) + Av(k+1), \tag{3}$$

where

$$F = \begin{bmatrix} 1 & 0 & T & 0 \\ 0 & 1 & 0 & T \\ 0 & 0 & 1 & 0 \\ 0 & 0 & 0 & 1 \end{bmatrix}, \text{ and } A = \begin{bmatrix} 0.5T^2 & 0 \\ 0 & 0.5T^2 \\ T & 0 \\ 0 & T \end{bmatrix}.$$

The vector $v(k+1)$ represents unknown accelerations as zero-mean Gaussian noise with covariance $Q_v = \sigma_v^2 I$, and $x(k)$ is the target state for the k-th snapshot. Finally, T is the time interval between successive snapshots.

2.2 Energy Consumption Model

This paper models the energy consumed for transmitting l bits over d meters in a multipath environment as

$$E = l \cdot \epsilon_{amp} \cdot d^4,$$

where ϵ_{amp} is a constant to represent the energy expense of engaging the power amplifiers to transmit sufficient signal power for delivery of one bit over a range of d meters. This transmission model was derived from the model used in (Heinzelman and Chandrakasan 2002), and it assumes that the energy usage is dominated by the radio rather than the computer (Raghunathan et al. 2002). Therefore in this paper we only consider how much energy is consumed due to radio transmission.

Over a single snapshot how energy is consumed depends on how activation decision is made. In this paper, the activation decision is performed in a decentralized manner over the active set of nodes after currently obtained information is shared among the active set of nodes. To this end, each active node determines the next active set by evaluating a metric, and decides whether it remains active or whether it should wake-up and handoff information to inactive nodes that are member of the next active set. Therefore, the broadcast range should be just long enough to reach all the active nodes for information sharing and to reach the next active set for information handoff. Let $\mathcal{N}$ and $\mathcal{N}^*$ be the currently and next active node set, respectively. As a result, over a single snapshot, node i in $\mathcal{N}$ consumes $\epsilon d^4_{i,\mathcal{N}^*}$

for information handoff to $\mathcal{N}^*$, and node j in $\mathcal{N}^*$ consumes $\epsilon d_{j,\mathcal{N}^*}^4$ for information sharing, where $\epsilon = l \cdot \epsilon_{amp}$,

$$d_{i,\mathcal{N}} = \max_{j \in \mathcal{N}} \{d_{i,j}\},$$

and $d_{i,j}$ is the distance between node i and node j.

2.3 Geometry-based (GB) Metric

For the purpose of minimizing the estimation error, Kaplan proposed a geometry-based (GB) objective function to select the desired number of active nodes (Kaplan 2006a,b). The Kalman-based root mean squared (RMS) position error with prior covariance information is used as the objective function. The state estimates and error covariances are updated via the extended Kalman filter where the bearing measurement is assumed to depend only on target position. Therefore the updated covariance, in a form of information, is explicitly expressed as

$$\mathbf{J}_f(\mathcal{N}) = \mathbf{J}_p + \begin{pmatrix} \mathbf{J}_m(\mathcal{N}) & \mathbf{0_2} \\ \mathbf{0_2} & \mathbf{0_2} \end{pmatrix}, \tag{4}$$

where

$$\mathbf{J}_m(\mathcal{N}) = \sum_{i \in \mathcal{N}} \frac{1}{\sigma_i^2} \frac{1}{r_i^2} \begin{pmatrix} \sin^2 \phi_i & -\sin \phi_i \cos \phi_i \\ -\sin \phi_i \cos \phi_i & \cos^2 \phi_i \end{pmatrix},$$

and r_i and ϕ_i are the 2D polar coordinates of the vector from the i-th node to the predicted target location. Then the posterior RMS position error is written as

$$\rho(\mathcal{N}) = \sqrt{\text{trace}([\mathbf{J}_f^{-1}(\mathcal{N})]_{1:2,1:2})}, \tag{5}$$

where $[\mathbf{A}]_{i:j,k:l}$ represents the $(j-i+1) \times (l-k+1)$ subblock of $\mathbf{A}$ and $\mathbf{J}_p$ represents the predicted error information, i.e., the inverse of predicted error covariance. Obviously, $\rho(\mathcal{N})$ is a function of the node set $\mathcal{N}$ and the predicted target state.

2.4 Partial Network Knowledge

For large sensor networks, a perfect assumption that a node knows every other node's location becomes impractical. In practice, a node will only keep a table about its neighbors, i.e., the set of nodes within a distance of r_{nei}. Furthermore, it is reasonable for the nodes within earshot of the active set to be able to store information about the active nodes. Let $\mathcal{N}_{nei}(i) = \{j | d_{i,j} \leq r_{nei}, i \neq j\}$ be the neighbor node set of the i-th node. Assumably, the active nodes will provide battery level updates to the other nodes. How partial network knowledge affects node selection approaches is discussed in Section 3.

3 Energy-aware Node Selection Approach

This section discusses energy-aware node selection approaches to balance the localization accuracy in lieu of the energy costs. We focus on comparisons among different energy-related metrics to extend the tracking lifetime while maintaining a certain level of tracking accuracy. The acceptable level of tracking accuracy denoted by ρ_0 is user-defined. A subset of nodes that can meet this requirement is

$$\mathcal{C}_{\rho_0} = \{\mathcal{N} | \mathcal{N} \subseteq \mathcal{N}_{known}; \rho(\mathcal{N}) \leq \rho_0\}, \tag{6}$$

where $\mathcal{N}_{known}$ must reflect the available network knowledge and the power strength of the currently active nodes $\mathcal{N}_0$ (Le et al. 2006), and $\rho(\mathcal{N})$ denotes the posterior position RMS error by (5). Explicitly

$$\mathcal{N}_{known} = \{\{\cap_{i \in \mathcal{N}_0} \mathcal{N}_{nei}(i)\} \cup \mathcal{N}_0\} \cap \mathcal{N}^{mr}, \tag{7}$$

where the common reachable node set of the active nodes is

$$\mathcal{N}^{mr} = \bigcap_{j \in \mathcal{N}_0} \left\{ i | d_{i,j} \leq \sqrt[4]{\frac{p_j}{\epsilon}} \right\}, \tag{8}$$

p_j is the j-th node's remaining power level. One could maximize or minimize an energy-related metric to obtain the active set $\mathcal{N}^*$ for the subsequent snapshot:

$$\mathcal{N}^* = \arg \max_{\mathcal{N} \in \mathcal{C}_{\rho_0}} \mathbf{E}(\mathcal{N}), \tag{9}$$

where $\mathbf{E}(\mathcal{N})$ is either $\mathbf{CL}(\mathcal{N})$, $\mathbf{NCL}(\mathcal{N})$, or $\mathbf{EB}(\mathcal{N})$ in the following subsections.

3.1 Energy-based (EB)

The traditional energy-based metric is the energy usage required to communicate data (Williams et al. 2005). Since in our energy consumption model energy is consumed due to information sharing and handoff, then the energy usage over a single snapshot could be

$$\mathbf{EB}(\mathcal{N}) = \sum_{i \in \mathcal{N}_0} \epsilon d_{i,\mathcal{N}}^4 + \sum_{i \in \mathcal{N}} \epsilon d_{i,\mathcal{N}}^4. \tag{10}$$

Although it reflects the total amount of energy usage for information handoff from $\mathcal{N}_0$ to $\mathcal{N}$, and information sharing among $\mathcal{N}$, this metric by (10) neglects nodes' battery levels.

3.2 Current Lifetime (CL)

Given a node i and a node set $\mathcal{N}$ that node i must share data with, the number of snapshot cycles that node i could run, known as CL of node i, could a function of node i's battery level and energy usage for sharing: $\frac{p_i}{\epsilon d_{i,\mathcal{N}}^4}$. Therefore, a current lifetime metric could be defined as

$$\mathbf{CL}(\mathcal{N}) = \lambda \min_{i \in \mathcal{N}} \frac{p_i}{\epsilon d_{i,\mathcal{N}}^4} + (1-\lambda) \min_{i \in \mathcal{N}_0} \frac{p_i - \epsilon d_{i,\mathcal{N}}^4}{\epsilon d_{i,\mathcal{N}_0}^4}, \tag{11}$$

The parameter λ controls the relative weighting of two terms representing the CLs of node set $\mathcal{N}$ and $\mathcal{N}_0$ for

1) data sharing and 2) after information handoff, respectively. One way to obtain a better λ to balance the energy usages of data handoff and sharing is to sample λ from 0 to 1. Since in the CL metric we include the battery level, we could avoid the overuse of essential nodes to achieve load balancing.

3.3 Nonlinear Current Lifetime (NCL)

Instead of using λ to weight the CLs of node set $\mathcal{N}$ and $\mathcal{N}_0$, we could treat node set $\mathcal{N} \cup \mathcal{N}_0$ as a whole and define its CL:

$$\mathbf{NCL}(\mathcal{N}) = \min_{i \in \mathcal{N} \cup \mathcal{N}_0} f(i),$$
$$f(i) = \left\{ \begin{array}{cc} \frac{p_i - \epsilon d_{i,\mathcal{N}}^4}{\epsilon d_{i,\mathcal{N}_0}^4} & \text{if } i \in \mathcal{N}_0 \setminus (\mathcal{N} \cap \mathcal{N}_0) \\ \frac{p_i}{\epsilon d_{i,\mathcal{N}}^4} - 1 & \text{if } i \in \mathcal{N} \cap \mathcal{N}_0 \\ \frac{p_i}{\epsilon d_{i,\mathcal{N}}^4} & \text{if } i \in \mathcal{N} \setminus (\mathcal{N} \cap \mathcal{N}_0) \end{array} \right\}. \quad (12)$$

The NCL metric not only keeps the virtue of CL metric(capable of avoiding the overuse of essential nodes by considering nodes' battery level), but also avoids the use of balance factor λ.

3.4 Greedy Search

Once the metrics are built, we need a fast search algorithm for the solution that is the subsequently active node set. Exhaustively enumerating the node sets with different sizes to meet the tracking accuracy ρ_0 to get the optimal solution by (9) is prohibitive. So we use the "add one node at a time" strategy, known as Greedy search, to build an nonempty candidate space containing sets that meet ρ_0. Fig. 1 shows the steps of the Greedy search method. Instead of exhaustively enumerating all the node sets with a certain length, say M_d, the Greedy search adds one more node into the existing suboptimal M_d-node set $\mathcal{N}_m$(Step 4) and stops when $\mathcal{C}_{cand}$ is not empty. The computational complexity via Greedy search consists of exhaustively evaluating 2-node sets, $\mathbf{O}(N^2)$, and adding one at a time, $\mathbf{O}((|\mathcal{N}^*| - 2)N)$.

In the Greedy search, M_d represents the number of active nodes for the next snapshot. Once an active set of size M_d is found that satisfies the localization constraint ρ_o, then the Greedy search terminates. If one is employing the EB or CL metric, further iteration of the Greedy search will not lead to a better active set due to the following theorem.

Theorem 1 *If* $\mathcal{N}_1 \subseteq \mathcal{N}_2$ *and* $\rho(\mathcal{N}_1) \le \rho_0$*, then* $\rho(\mathcal{N}_2) \le \rho(\mathcal{N}_1) \le \rho_0$*,* $\mathbf{EB}(\mathcal{N}_1) \le \mathbf{EB}(\mathcal{N}_2)$*, and,* $\mathbf{CL}(\mathcal{N}_2) \le \mathbf{CL}(\mathcal{N}_1)$.

Proof: See Appendix.

Clearly, Theorem 1 justifies the use of $\mathcal{C}_{cand} \neq \emptyset$ as the stopping criteria for the Greedy search (see Fig. 1) when the EB or CL metric is embedded into the multi-objective optimization. The Greedy search can still be employed for the NCL metric even though the stopping criteria does not guarantee that a better solution will be found by a larger M_d. Future work will investigate other possible stopping criteria for the NCL metric.

1. $M_d = 2$, $N = |\mathcal{N}_{known}|$, where $\mathcal{N}_{known}$ is given by (7);
2. enumerate all M_d-node subsets to form $\mathcal{C} = \{\mathcal{N} | |\mathcal{N}| = M_d; \mathcal{N} \subseteq \mathcal{N}_{known}\}$,
   and $\mathcal{C}_{cand} = \{\mathcal{N} | \mathcal{N} \in \mathcal{C}; \rho(\mathcal{N}) \le \rho_0\}$;
3. $\mathcal{N}_m = \arg\min_{\mathcal{N} \in \mathcal{C}} \rho(\mathcal{N})$;
4. while $M_d \le N$ & $\mathcal{C}_{cand}$ is empty,
   $\mathcal{C} = \{\mathcal{N} | \mathcal{N} = \mathcal{N}_m \bigcup \{j\}; j \in \mathcal{N}_{known} \setminus \mathcal{N}_m\}$;
   $\mathcal{C}_{cand} = \{\mathcal{N} | \mathcal{N} \in \mathcal{C}; \rho(\mathcal{N}) \le \rho_0\}$;
   $\mathcal{N}_m = \arg\min_{\mathcal{N} \in \mathcal{C}} \rho(\mathcal{N})$;
   $M_d = |\mathcal{N}_m|$;
   end
5. $\mathcal{C}_g = \mathcal{C}_{cand}$;
6. $\mathcal{N}^* = \arg\max_{\mathcal{N} \in \mathcal{C}_g} \mathbf{E}(\mathcal{N})$;

Figure 1: Greedy search for the joint metric optimization.

4 Experiments

In the simulations, a target traverses along a straight line at a constant speed of 10m/s in a 2km×1km field shown in Fig. 2. The time interval for updating the tracker is set to 1 second. The goal here is to measure how accurate the tracking estimates are over the lifetime of the network. We define the effective lifetime as the earliest point when all the reachable nodes can meet the error threshold ρ_0, that is when $\rho(\mathcal{N}_{known}) \ge \rho_0$.

Fig. 3 shows the performance using (11). Figs. 3(a) and (b) plot average RMS error versus lifetime for different values of r_{nei} for $\lambda = 1$ and $\lambda = 0$, respectively. Each point on the curves in Figs. 3(a) and (b) represent a different value of ρ_0, where ρ_0 varies from 10m to 70m. As ρ_0 increases, so does the localization error (and usually the lifetime). Each point on the curve is the result of averaging over 1000 Monte Carlo simulations (100 Monte Carlo runs for 10 different configurations of UGS networks). Fig. 3(c) provides the average lifetime performance as a function of λ when $\rho_0 = 30$m. As expected, a looser constraint on the position accuracy leads to a longer network lifetime. For a given position error, the lifetime is longer when $\lambda = 1$ than when $\lambda = 0$ for a given value of ρ_o and r_{nei}. In other words, it is more important to consider the data sharing cost

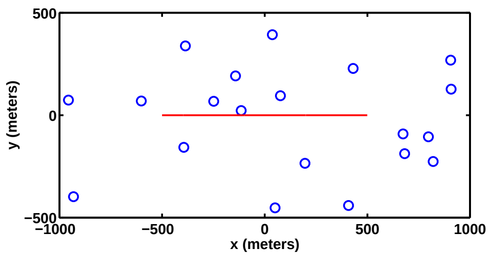

Figure 2: Node configuration with twenty nodes where $\circ$ denotes the node and the solid line denotes the true target track along which a target comes back and forth for an infinite time.

than the cost for a dormant node to join the active set. However, when $\lambda = 1$, the incorporation of global knowledge, i.e., large r_{nei}, can actually lead to shorter lifetimes as compared to smaller r_{nei} because the active nodes can choose a different set of faraway active nodes for the next snapshot when the handoff costs are neglected. In Fig. 3(a), $r_{nei} = 800$m is best while in Fig. 3(b), $r_{nei} = 1200$m is best. For most values of r_{nei}, the lifetime is actually longest for λ slightly larger than zero. Therefore, both the data sharing and handoff costs must be considered in (11).

Fig. 4 shows the performances of different energy-related metrics denoted by (10), (11) and (12) as a function of r_{nei} for a given $\rho_0 = 30$m. The available neighbor information r_{nei} varies at 0, 600, 800, 900, and 1200m. Again, each point is the result of averaging over 1000 Monte Carlo simulations (10 different configurations of UGS networks and 100 Monte Carlos for each node configuration). Furthermore, the lifetime of each point on the CL curve is the best among the samples of λ. When r_{nei} is larger than 600m, the NCL is the best. The NCL is better than the CL because the NCL computes the minimum current lifetime among the nodes of the currently active node set and the next active node set instead of treating the current lifetimes of the currently active node set and the next active node set separately. The NCL is also better than the traditional EB metric because overuse of the essential nodes could be avoided when nodes' battery levels are taken into account in a metric. However the advantage of considering the battery levels in the CL over EB is not clear. The reason might be that the tradeoff between data sharing and handoff, i.e., λ, is not properly accounted for when ρ_0 is relatively small. We increase ρ_0 to see whether the CL could outperform the EB, and the result with increasing ρ_0 is shown in Fig. 5.

Fig. 5 shows the performances of different energy related metrics denoted by (10), (11) and (12) as a function of ρ_0 when $r_{nei} = 600$m. The error threshold ρ_0 varies at 30, 50, 70, 100, 150 and 200m. Again, each point is the result of averaging over 100 Monte Carlo simulations (10 different configurations of UGS networks and 10 Monte Carlos for each node configuration). We choose $\lambda = 0.5$ and λ=0.01 to plot the CL, and the lifetime of $\lambda = 0.5$ is longer than $\lambda = 0.01$, which is consistent with Fig. 3.c when $r_{nei} = 600$m. The figure shows that for looser accuracy tolerance, both the CL and NCL can extend the lifetime the of the network relative to the EB metric.

5 Conclusions and Future Work

We improved energy-related metrics to extend the effective tracking lifetime under the constraint of a user-defined tracking error. The CL/NCL accounts for not just the energy usage for information sharing and handoff, but also the battery levels of nodes, while the traditional EB metric is simply the energy usage over a single snapshot. Simulation results show that the CL/NCL metric provides longer lifetime than the EB metric under the larger error thresholds. Future work will compare the performance of the myopic optimization CL/NCL metrics against nonmyopic scheduling for the M-step horizon energy usage, i.e., EB, metric. We also plan to investigate alternative efficient searching and stopping criteria for the EB metric.

6 Appendix

Proof of Theorem 1

Proof: Proof of $\rho(\mathcal{N}_2) \leq \rho(\mathcal{N}_1)$ could be seen in (Le et al. 2006).

Suppose that we add one more node m into $\mathcal{N}_1$ to form $\mathcal{N}_2 = \{m, \mathcal{N}_1\}$. Then we have

$$\begin{aligned}\mathbf{EB}(\mathcal{N}_2) &= \sum_{i\in\mathcal{N}_0} d^4_{i,\mathcal{N}_2} + \sum_{i\in\mathcal{N}_2} d^4_{i,\mathcal{N}_2} \\ &= \sum_{i\in\mathcal{N}_0} d^4_{i,\mathcal{N}_2} + \sum_{i\in\mathcal{N}_1} d^4_{i,\mathcal{N}_2} + d^4_{m,\mathcal{N}_2}.\end{aligned}$$

Since $d_{i,\mathcal{N}_2} = \max\{d_{i,\mathcal{N}_1}, d_{i,m}\} \geq d_{i,\mathcal{N}_1}$, then, $\mathbf{EB}(\mathcal{N}_1) \leq \mathbf{EB}(\mathcal{N}_2)$.

In addition,

$$\begin{aligned}\mathbf{CL}(\mathcal{N}_2) &= \lambda \min_{i\in\mathcal{N}_2} \frac{p_i}{\epsilon d^4_{i,\mathcal{N}_2}} + (1-\lambda) \min_{i\in\mathcal{N}_0} \frac{p_i - \epsilon d^4_{i,\mathcal{N}_2}}{\epsilon d^4_{i,\mathcal{N}_0}} \\ &= \lambda \min \left\{ \min_{i\in\mathcal{N}_1} \frac{p_i}{\epsilon d^4_{i,\mathcal{N}_2}}, \frac{p_m}{\epsilon d^4_{m,\mathcal{N}_1}} \right\} \\ &\quad +(1-\lambda) \min_{i\in\mathcal{N}_0} \frac{p_i - \epsilon d^4_{i,\mathcal{N}_2}}{\epsilon d^4_{i,\mathcal{N}_0}} \\ &\leq \lambda \min_{i\in\mathcal{N}_1} \frac{p_i}{\epsilon d^4_{i,\mathcal{N}_2}} + (1-\lambda) \min_{i\in\mathcal{N}_0} \frac{p_i - \epsilon d^4_{i,\mathcal{N}_2}}{\epsilon d^4_{i,\mathcal{N}_0}}\end{aligned}$$

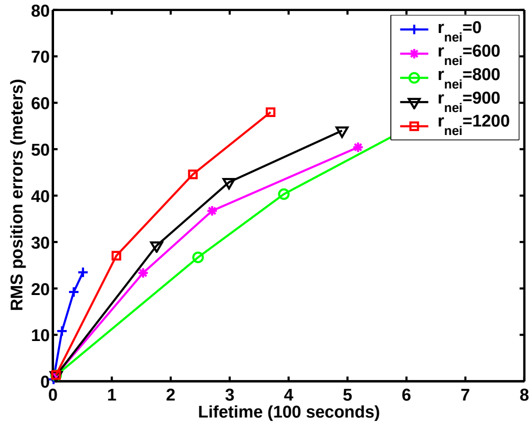

(a)

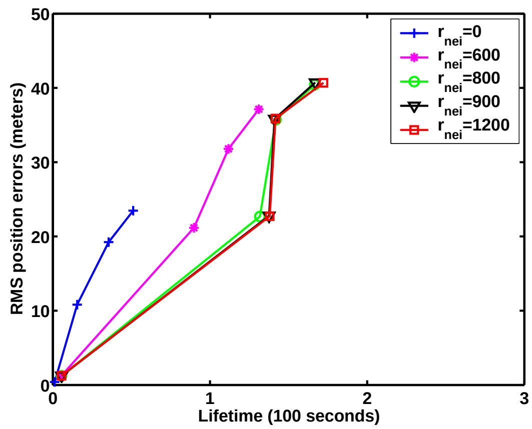

(b)

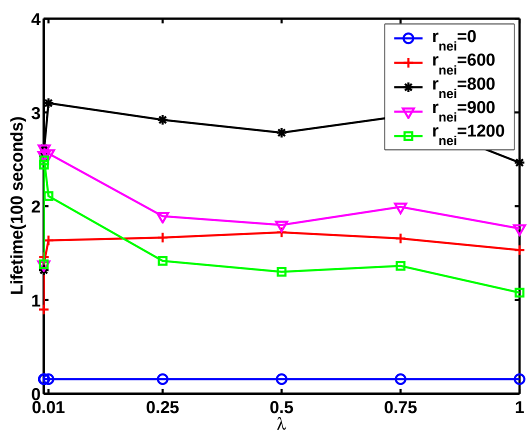

(c)

Figure 3: Performance of node selection using (11): (a) RMS position error vs. lifetime when $\lambda = 1$, (b) RMS position error vs. lifetime when $\lambda = 0$, and (c) lifetime vs. λ when $\rho_0 = 30$m.

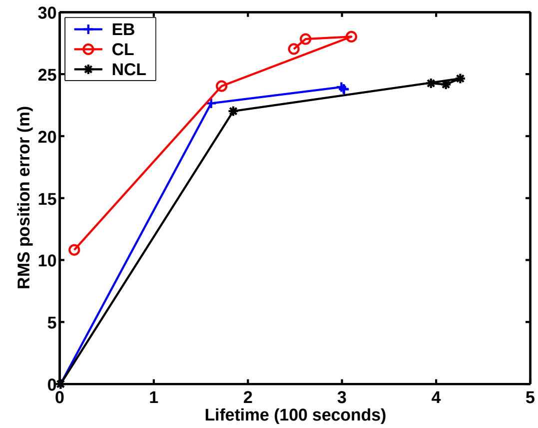

Figure 4: Performance of node selections using different energy-related metrics as a function of r_{nei} when $\rho_0 = 30$m.

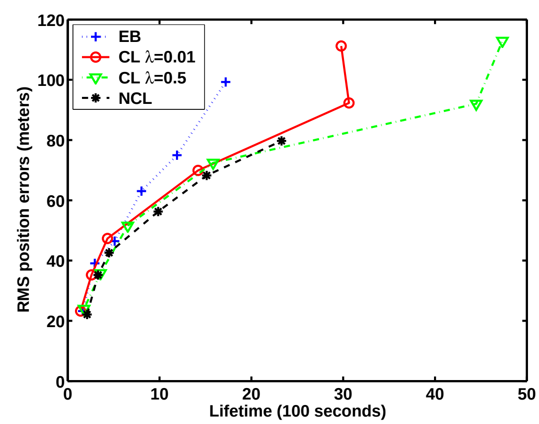

Figure 5: Performance of node selections using different energy-related metrics as a function of ρ_0 when $r_{nei} = 600$m.

$$\leq \quad \lambda \min_{i \in \mathcal{N}_1} \frac{p_i}{\epsilon d_{i,\mathcal{N}_1}^4} + (1-\lambda) \min_{i \in \mathcal{N}_0} \frac{p_i - \epsilon d_{i,\mathcal{N}_1}^4}{\epsilon d_{i,\mathcal{N}_0}^4}.$$

Therefore, $\mathbf{CL}(\mathcal{N}_2) \leq \mathbf{CL}(\mathcal{N}_1)$.

References

Chhetri, A. S., D. Morrell, and A. Papandreou-Suppappola: 2004, Efficient search strategies for non-myopic sensor scheduling in target tracking. *Proc.of the Thirty-Eighth Asilomar Conference on Signals, Systems and Computers*, volume 2, 2106–2110.

Filipov, A., N. Srour, and M. Falco: 2004, Distributed and disposable sensors at ARL and the ASCTA. *Proc. of IEEE Aerospace Conference*, Big Sky, MT.

Heinzelman, W. B. and A. P. Chandrakasan: 2002, An application-specific protocol architecture for wireless microsensor networks. *IEEE Trans. on Wireless Communications*, **1**, 660–669.

Kaplan, L. M.: 2006a, Global node selection for target localization in a distributed sensor network. *IEEE Trans. on Aerospace and Electronic Systems*, **1**, 113–135.

— 2006b, Local node selection for localization in a distributed sensor network. *IEEE Trans. on Aerospace and Electronic Systems*, **1**, 136–146.

Kaplan, L. M. and Q. Le: 2005, On exploiting propagation delays for passive target localization using bearings-only measurements. *Journal of Franklin Institute*, **342**, 193–211.

Le, Q., L. M. Kaplan, and J. H. McClellan: 2006, Multiobjective energy-aware node selection. *Proc. of IEEE Aerospace Conference*, Big Sky, MT.

Raghunathan, V., C. Schurgers, S. Park, and M. Srivastava: 2002, Energy-aware wireless microsensor networks. *IEEE Signal Processing Magazine*, **19**, 40–50.

Williams, J. L., J. W. Fisher III, and A. S. Willsky: 2005, An approximate dynamic programming approach to a communication constrained sensor management problem. *Proc. Eighth International Conference of Information Fusion*.